



Publication Year	2016
Acceptance in OA	2020-07-07T12:15:39Z
Title	Developments in fiber-positioning technology for the WEAVE instrument at the William Herschel Telescope
Authors	Schallig, Ellen, Lewis, Ian J., Gilbert, James, Dalton, Gavin, Brock, Matthew, Abrams, Don Carlos, Middleton, Kevin, Aguerri, J. Alfonso L., BONIFACIO, PIERCARLO, Carrasco, Esperanza, Trager, Scott C., VALLENARI, Antonella
Publisher's version (DOI)	10.1117/12.2231626
Handle	http://hdl.handle.net/20.500.12386/26365
Serie	PROCEEDINGS OF SPIE
Volume	9908

PROCEEDINGS OF SPIE

[SPIDigitalLibrary.org/conference-proceedings-of-spie](https://spiedigitallibrary.org/conference-proceedings-of-spie)

Developments in fiber-positioning technology for the WEAVE instrument at the William Herschel Telescope

Schallig, Ellen, Lewis, Ian, Gilbert, James, Dalton, Gavin, Brock, Matthew, et al.

Ellen Schallig, Ian J. Lewis, James Gilbert, Gavin Dalton, Matthew Brock, Don Carlos Abrams, Kevin Middleton, J. Alfonso L. Aguerri, Piercarlo Bonifacio, Esperanza Carrasco, Scott C. Trager, Antonella Vallenari, "Developments in fiber-positioning technology for the WEAVE instrument at the William Herschel Telescope," Proc. SPIE 9908, Ground-based and Airborne Instrumentation for Astronomy VI, 99087U (9 August 2016); doi: 10.1117/12.2231626

SPIE.

Event: SPIE Astronomical Telescopes + Instrumentation, 2016, Edinburgh, United Kingdom

Developments in fibre-positioning technology for the WEAVE instrument at the William Herschel Telescope

Ellen Schallig^a, Ian J. Lewis^{*a}, James Gilbert^{a,b}, Gavin Dalton^{a,c}, Matthew Brock^a, Don Carlos Abrams^d, Kevin Middleton^b, J. Alfonso L. Aguerri^e, Piercarlo Bonifacio^f, Esperanza Carrasco^g, Scott C. Trager^h, Antonella Vallenariⁱ

^aDept. of Physics, Keble Road, University of Oxford, OX1 3RH, UK; ^bRSAA, Mount Stromlo Observatory, Cotter Road, Weston Creek, ACT 2611, Australia; ^cRAL Space, Science and Technology Facilities Council, Rutherford Appleton Laboratory, Harwell Oxford, Didcot, Oxfordshire, OX11 0QX, UK; ^dIsaac Newton Group, 38700 Santa Cruz de La Palma, Spain; ^eInstituto de Astrofísica de Canarias, 38200 La Laguna, Tenerife, Spain; ^fGEPI, Observatoire de Paris, Place Jules Janssen, 92195 Meudon, France; ^gInstituto Nacional de Astrofísica, Óptica y Electrónica (INAOE, Mexico), Mexico, ^hKapteyn Instituut, Rijksuniversiteit Groningen, Postbus 800, NL-9700 AV Groningen, Netherlands, ⁱOsservatorio Astronomico di Padova, INAF, Vicolo Osservatorio 5, 35122, Padova, Italy

ABSTRACT

WEAVE is the next-generation wide-field optical spectroscopy facility for the William Herschel Telescope (WHT) on La Palma in the Canary Islands, Spain. It is a multi-object "pick-and-place" fibre-fed spectrograph with a 1000 fibre multiplex behind a new dedicated 2° prime focus corrector. The WEAVE positioner concept uses two robots working in tandem in order to reconfigure a fully populated field within the expected 1 hour dwell-time for the instrument (a good match between the required exposure times and the limit of validity for a given configuration due to the effects of differential refraction). In this paper we describe some of the final design decisions arising from the prototyping phase of the instrument design and provide an update on the current manufacturing status of the fibre positioner system.

Keywords: Fibre Spectroscopy, WHT, WEAVE, Robotic Positioners, High Multiplex Spectroscopy

1. INTRODUCTION

The WEAVE spectrograph and its purpose are described in detail in Dalton et al.¹ The WEAVE prime focus has a 2° field of view which can be populated by up to 1000 optical fibres to feed light to the spectrographs, plus 8 coherent fibre bundles feeding an autoguider. The fibre positioner contains two fieldplates and two sets of fibres so that, while one plate is in the focal plane, the other can be re-configured by a pair of fibre-positioning robots. To move to a new field, the plates are swapped over and the spectrographs and autoguiders switched to the other set of fibres. In order to maximise the efficiency of the instrument this means that re-configuring a fibre layout for a new field has to be achievable in about 60 minutes, the length of a typical dwell time on a target field. In this paper we provide an update on the design after the final design review process and report on some of the prototyping work undertaken. Finally, we provide an update on the assembly schedule.

*ijl@astro.ox.ac.uk; phone +44 1865 273340

2. FINAL DESIGN DECISIONS

2.1 Updated gripper design

The final gripper design is based on a commercial two-fingered gripper unit from Schunk GmbH & Co with custom fingers to grip the handle of the fibre buttons. The back-illuminated optical fibre is viewed by a small CCD camera via an optical relay.

We have tested the repeatability and accuracy of the commercial gripper unit fitted with our custom jaws while handling some of the WEAVE prototype magnetic buttons. These tests have confirmed that the repeatability is at the level of a few microns².

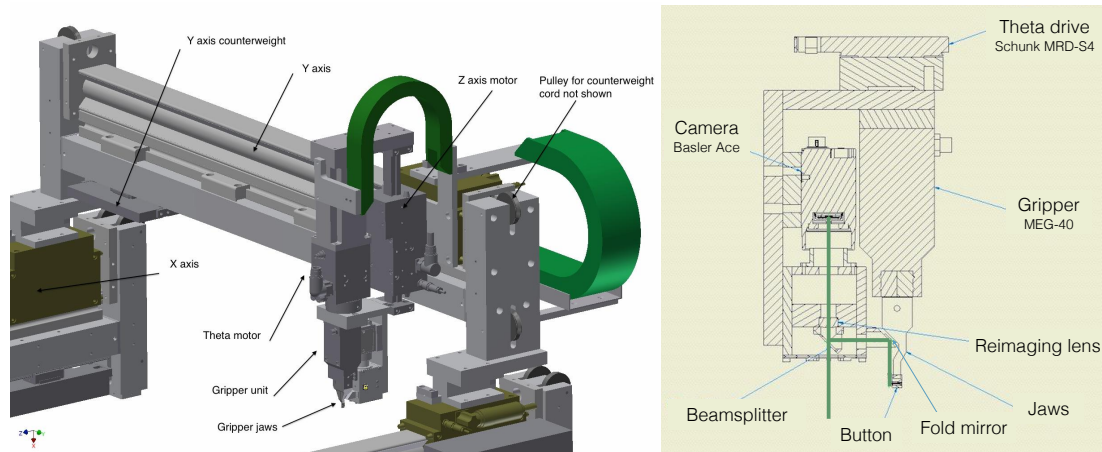


Figure 1 Robot assembly and cross section of gripper and camera unit.

The gripper camera optical system uses a beamsplitter to give two different foci. The first focus is aligned with the optical fibre button when it is securely grasped in the gripper jaws. The second focus is aligned so that the camera can see an in-focus view of the fieldplate when the gripper unit is raised safely above the height of any fibre buttons. This is used for measuring the reference marks in the fieldplate, locating fibres on first starting up and during troubleshooting for lost fibres. To aid in this there are also built in LED floodlights in the base of the gripper, which can be turned on when required.

2.2 Flexure modelling and compensation

As part of the design process extensive use was made of finite-element analysis techniques to model the likely deflections due to gravity of the robot positioner during observations on the telescope. This modelling has to include variations due to telescope elevation and prime focus rotator angle. During the modelling it quickly became apparent that a mechanical design with minimal flexure was not achievable within the size and mass budget available; rather we sought to minimise flexure and provide a means to calibrate it during observations.

Each fieldplate has a reference grid built into its surface. The robots measure the grid and compare their sets of x - y coordinates against a reference set to calculate shifts and rotations of the fieldplate and also perpendicularity, straightness and flexure of the robot axes. These can then be removed with a software transformation of the encoder positions to real-world positions. The change in this flexure is small during the course of a reconfiguration and is allowed for in the positioning error budget.

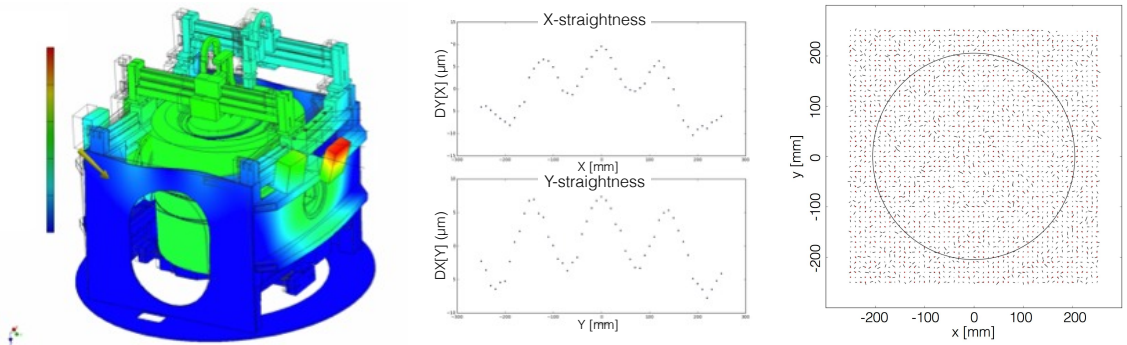


Figure 2 Flexure modelling, characterisation and correction. The FEA model was used to generate a simulation of a measured reference grid with the required shifts, shear, rotation and flexure. These terms were then evaluated from the ‘measured’ grid including removing the axis straightness and flexure. The resulting transformation was then applied to the original measurements and compared to the input reference grid. The resulting residuals were typically $3.1\mu\text{m}$ rms, with no remaining systematic structure.

2.3 Final magnetic fibre button designs

Each of the optical fibre probes is terminated in the focal plane in a small magnetic button. This button attaches the fibre probe to the fieldplate which is positioned a nominal 2.4mm behind the telescope focal plane, and is used by the robot to re-position the fibre probes on the fieldplate.

There are three different types of fibre probe: guide fibres, MOS fibres and mini-IFU (or mIFU). Each type has its own magnetic button design in order to keep all three button types par-focal since they have different optical paths and the guide fibres are required to be used with both the MOS fibres and the mIFU probes.

The MOS and guide fibre buttons are both 5mm long and house a NdFeB permanent magnet in the base. Both have a 2° tilt for the axis of the optical fibre ferrule, this being close to the average non-telecentricity of the chief ray across the focal plane. The only practical difference is a very slight height offset between the optical fibres, because the MOS buttons have a focal ratio conversion lens built into the micro-prism and the guide fibres have a simple 90° prism. The mIFU button is much larger and has a separate field lens to provide adequate image quality over a wider field of view for the 37-fibre integral field unit.

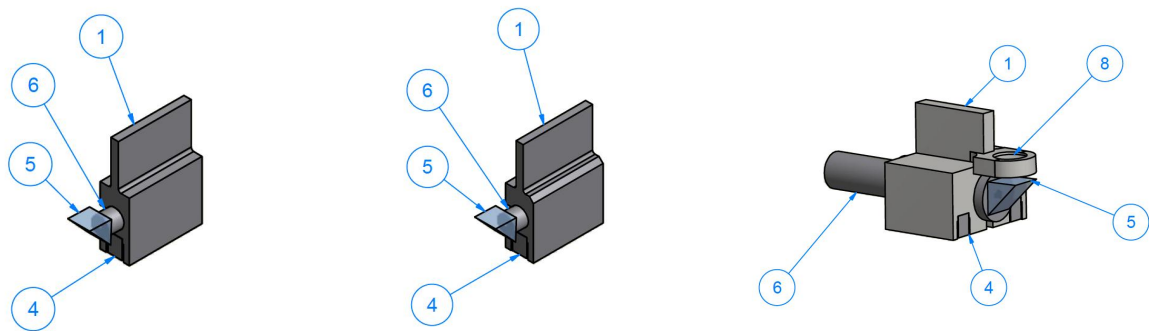


Figure 3 Schematic of MOS, guide and mIFU fibre magnetic buttons. In each case part 1 is the button housing made from magnetic stainless steel, 4 is a NdFeB permanent magnet, 5 is a prism, 6 is the fibre ferrule and for the mIFU button 8, is the separate field lens.

3. TECHNOLOGY PROTOTYPING

3.1 Fast accurate fibre centre-finding

A clear requirement for “pick-and-place” fibre-positioning systems is that we must be able to quickly measure the actual fibre position. This is normally achieved by measuring an image of the back-illuminated fibre and combining this with the known position of the camera when taking the image. We require a fibre centre-finding method that is fast, robust against varying illumination and accurate to sub-pixel levels. Simple centroiding may be the method of choice if the fibre is unresolved and the fibre image is dominated by the PSF of the camera optics. However, for resolved images such as used in WEAVE a centroid is not a robust method. This is illustrated in figure 4a which shows how an uneven core illumination pattern can influence the centroid calculation.

The first step in almost all centre-finding techniques is an initial pre-processing stage. Each new fibre measurement begins with a digital frame from one of the two fibre measurement cameras consisting of an image 1280x960 pixels in size. The science fibres will appear as 22.5pixel diameter spots and therefore it is possible for multiple spots to be visible in cases where neighbouring fibre buttons are close by.

We use an intensity histogram of the image to calculate a threshold value and to reject saturated images. Next a simple centroid of the image is calculated for all pixels above the threshold with equal weight. Then all pixels above the threshold have their pixel moment calculated with respect to the centroid location. The sum of the moments can be used to identify the presence of multiple images, see figure 4b.

If the sum of moments is too high then the image is cropped about its centre until only one image is present. Finally, the remaining image is cropped around the fibre of interest, ready for the second stage of processing.

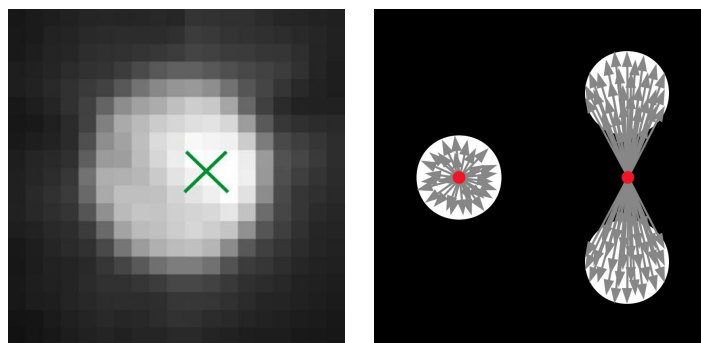


Figure 4 a) Simple centroid showing the effect of illumination pattern on centroid result for a resolved image b) Using the sum of moments about a simple centroid to detect the presence of more than one fibre in the image.

The drawbacks of the simple centre-of-mass centroiding method have already been discussed earlier in this section. They chiefly concern the centroid method bias to brighter areas of an image and hence its dependence on flawless fibre images. Therefore, three other methods have been considered to test their performance with images of a potentially lesser quality: a parabolic fit, cross-correlation and a simplified cross-correlation method.

A parabolic centroiding technique fits a second-order polynomial to separate 1-d collapsed images of the fibre along the x - and y -axes. This works well but is relatively slow compared to a simple centroid and is susceptible to the correct determination of a threshold intensity or a background gradient.

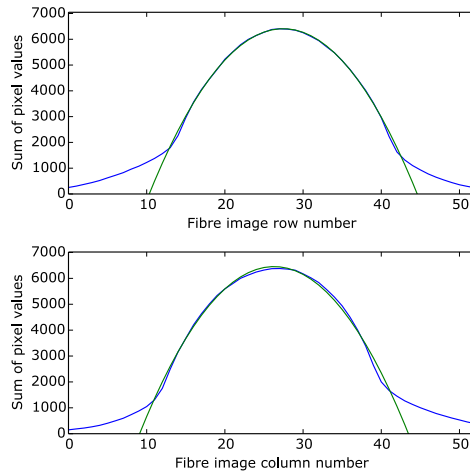


Figure 5 The parabolic fit method fits two second-order polynomials to 1-d versions of the fibre image collapsed along the pixels and rows.

The cross-correlation method uses prior knowledge of the expected size and shape of the fibre image to optimise the centroiding process. The prototype of this algorithm uses a modified 2-d Fourier space cross-correlation algorithm² to compare the fibre image with an ideal image consisting of a white circle on a black background. This method has the advantage that it does not rely on a particular threshold value, but its performance does depend on the correct fibre diameter being chosen. Tests of fibre images at the centre and edge of the camera field of view showed that for a known fibre size it was far better to under-estimate the size of the fibre by a few per cent than to over-estimate because of the expected variation in fibre core size due to manufacturing tolerances (Polymicro FBP 85/105/120 has a core size specified at $85 \pm 3\mu\text{m}$). This method also performed very well (accuracy and robustness) but was even slower than the parabolic fit method.

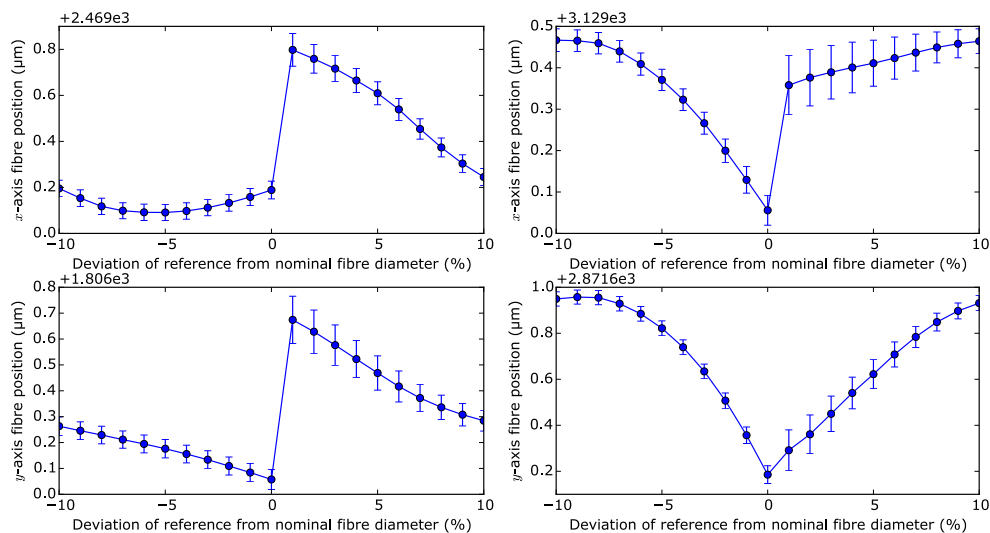


Figure 6 Effect of choice of reference circle diameter for the cross-correlation method. Two sets of cross-correlation results are shown: on the left the fibre is near the centre of the camera image, on the right the fibre is located near the edge of the camera image. The consequences of a non-optimal diameter are less severe for an undersized reference image and near the centre of the camera image.

A new algorithm, named the biscuit cutter method, has been developed² with the aim of achieving the results of the cross-correlation method above but in a fraction of the time. This method again makes use of prior knowledge of the fibre image size to create a series of pixel masks with values either 0 (outside the circle of size defined by the fibre size) or 1 (inside the circle). These masks are used to sum the pixels within the mask before moving the mask by a pixel and repeating this until a maximum in both x and y is achieved. To avoid the repeat calculations of unchanging pixels a series of difference masks can be calculated. Then after the first full image weight has been calculated, subsequent images only require the application of a difference mask. At this point we effectively have a very fast cross-correlation with single-pixel precision; to improve precision it is only necessary to produce difference masks representing equal subdivisions of a full pixel. The precision is set by the number of pixel subdivisions, which is only limited by the memory required to store the masks.

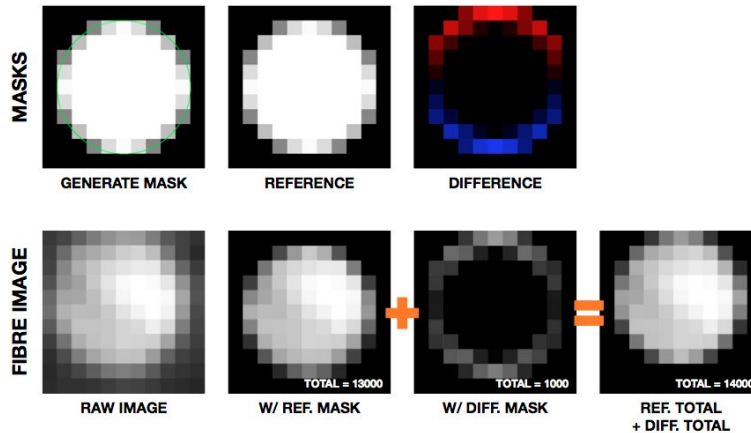


Figure 7 Biscuit cutter centre finding. In the first row a reference mask is generated along with a series of difference masks. In the second row the raw fibre image is multiplied with the mask and the resulting intensity summed. This result is then combined with the difference masks until the combination with the highest value is found. This can be repeated in both the x- and y-directions.

All four methods described above have been prototyped using identical test image sets and computer software. With the realistic image sizes and pixel scales all methods are able to produce acceptable results for good quality images, but assuming knowledge of the fibre core diameter the biscuit-cutter method enables very fast (comparable with the simple centroid method) and also robust and reliable fibre-centre finding. The absolute accuracy is quite difficult to measure, but a comparison of the results shows very good agreement between the cross-correlation and biscuit-cutter methods but indicates varying offsets of up to $3\mu\text{m}$ for fibres at the edge of the camera image for the centroid and parabolic fit methods compared to the other two methods.

	Offset due to tilted input illumination (μm)	Measurement noise (μm)	Speed (msec)
Pre-processing task			12.2
Simple centroid	0.2	0.07	0.14
Parabolic fit	0.21	0.05	2.39
Cross-correlation	0.18	0.05	98.7
“Biscuit cutter”	0.17	0.05	0.18

Table 1 Comparison of fibre centre-finding techniques.

3.2 “Pick-and-place” sequencing

The WEAVE positioner has a top level requirement to be able to reconfigure a complete field in under an hour. We have used simulations of the fibres configured into target fields and calculated the sequence of fibre movements to go from one field to the next field using two robots. This confirmed the total number of fibre movements required to be on average about 1800 movements. The two robots were idle for less than 5% of the time. If each robot has to move about 900 fibres, then the maximum time for each fibre is just under 3.5s.

The initial timing scheme was tested using the prototype robot gantry. The complete fibre movement sequence was broken up into a series of elements and each element was tested with real hardware. The time taken was measured over 100 cycles with the axis motors at their maximum practical velocity and acceleration. The breakdown of each stage is shown in figure 8 and the total duration is nearly 4.5s which exceeds the requirement. It would result in a full field reconfiguration time of nearly 20 minutes longer than the nominal target field exposure.

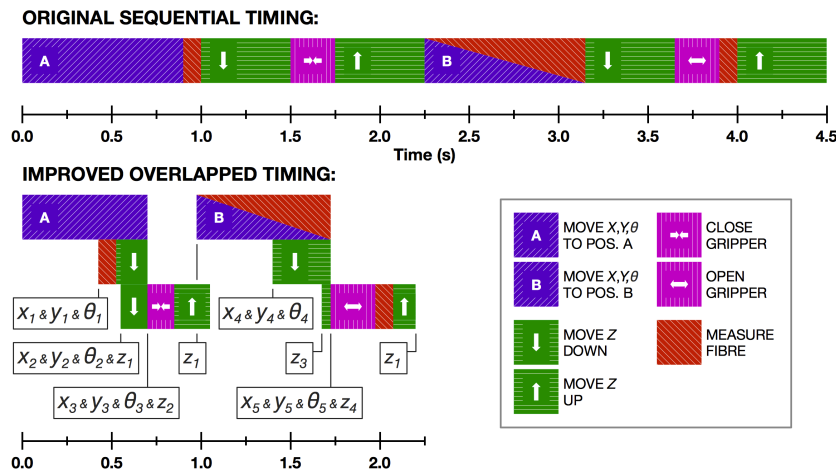


Figure 8 Breakdown of fibre movement strategies with timing information.

An improved fibre placement strategy has been developed by considering that the tightest positional tolerances on the robot movements are only necessary the moment before a fibre is released onto the fieldplate. Much more relaxed tolerances are acceptable when the robot is at a safe height above any other obstructions (fibres, buttons etc.). Tolerances become steadily tighter as the z-axis descends, leading to a hierarchical tolerance system that significantly reduces the time spent waiting for servo movements to complete.

We have tested this approach with the prototype and have demonstrated fibre placement times of less than 2.5s. Further improvements are possible, but as we can already fulfill the 60-minute reconfiguration requirement, further work will concentrate on robustness and reliability rather than absolute speed.

4. FIBRE RETRACTOR UNIT FINAL DESIGN AND TESTING

4.1 Retractor design

In the instrument 338 fibre retractors hold the final 2m of each of the 1900 fibres. Each retractor houses up to 6 fibres, which are kept tidy and free from twists and kinks by placing them under 13g / 0.13N of tension, using a constant-force spring-and-pulley system. See figures 9 and 10 for an overview. Each fibre has a 120µm outer diameter, loosely sleeved in a 500µm flexible PEEK tubing, seen in figure 11. The fibres are anchored in the retractor by pressing them in a closely fitting square groove. A length of 0.6m is in the retractor proper, 1.4m is kept in the spare-length box. This extra length is there for the inevitable repairs that will have to be done on the fibre ends during the instrument lifetime of operations.

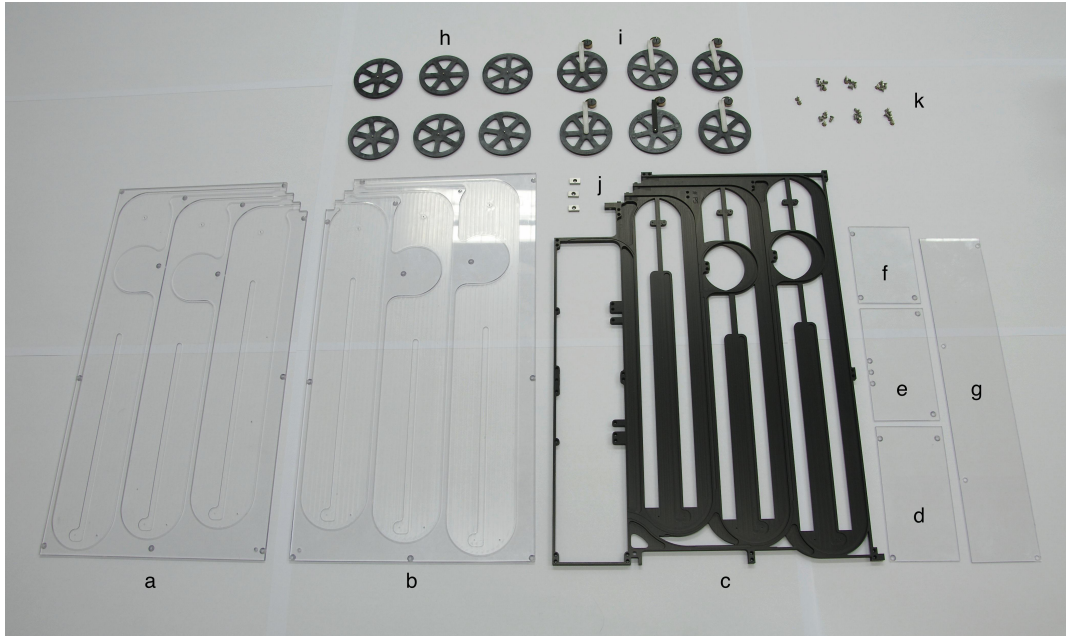


Figure 9 A single retractor unit component breakdown, a total of 106 individual parts: (a)-(b) covers, (c) centre plate, (d)-(g) spare-length-box covers, (h) fixed pulley assemblies, (i) moving pulleys with constant-force spring assemblies, (j) steel park porches, (k) fasteners.

The retractor central plate is made from aluminium, which is a departure from the previous polycarbonate prototypes. We found that the machining on the aluminium is much more precise than the polycarbonate, but the design had to be severely light-weighted to keep the overall mass the same. The aluminium is anodised black to prevent stray-light reflections. The covers are made of clear polycarbonate, as the machining does not need to be as precise for these components and it is useful to be able to see the fibre routing during assembly and testing.

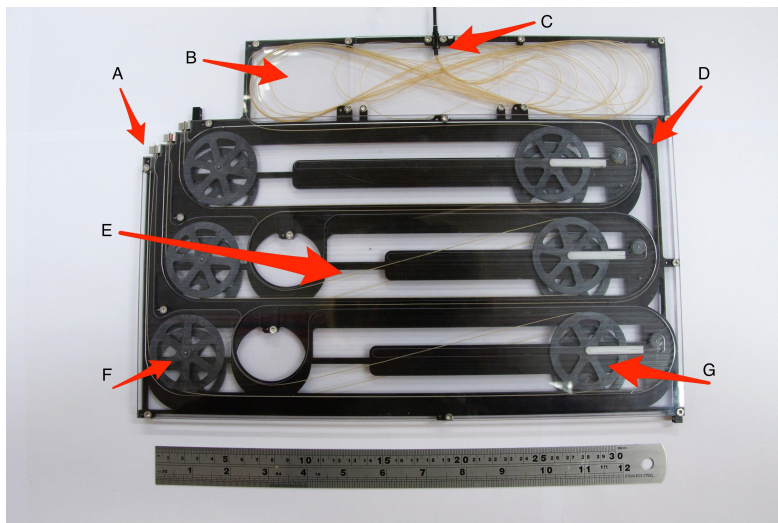


Figure 10 Assembled fibre retractor unit: (A) Fibre buttons, (B) Spare-length box, (C) Fibres exiting retractor, (D) Central plate with fibre secured in square groove, (E) Fibre under tension, (F) Fixed pulley, (G) Tensioned moving pulley.

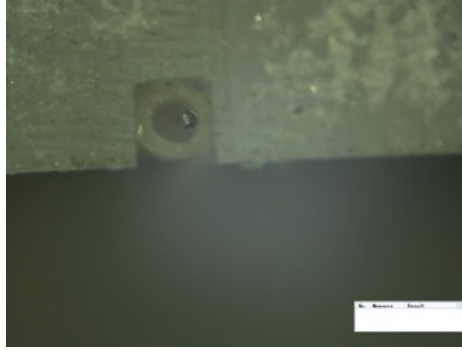


Figure 11 Retention of 120µm fibre in 0.5mm PEEK tube by pressing it into an accurately machined square groove.

An aluminium prototype was required to test the manufacturing process, ease of assembly, and durability. As we require 360 retractors (to include spares), streamlining manufacturing and assembly are important. This warranted a few design iterations during the prototyping phase. Assembly procedures were tested and timed at about 40 minutes per retractor.

4.2 Retractor testing

Lifetime testing was conducted to test the spring lifetime, wear on moving components and failures, such as slack in the fibre causing it to jump off the pulley. This consisted of pulling out and retracting a fibre for a number of cycles representative of a lifetime's operation. A lifetime is defined as 6 fields per plate per night over 70% of the total telescope time for five years, which amounts to about 8000 operations per fibre. An operation is defined as moving the fibre with the gripper back and forth over a distance of 175mm, coming to a complete stop at each end. This distance was chosen as 175mm is well over the average move distance² of about 137mm.

After 8000 operations the retractor was opened to check the status of the different components. A tiny amount of debris was found on one of the prototype wheels, which was due to a polishing effect from the turning of the wheel. This did not inhibit the correct operation of the pulley. The aluminium centre plate showed no signs of wear at all.

Another 10000 operations were completed with different accelerations. The fastest tested acceleration was 2ms^{-2} . The force on the fibre due to the spring was strong enough that there was no slack as it was going back into the retractor, even at the highest accelerations. There was no visible wear on the centre plate and other components, and no extra wear on the wheels.

The tests did show that care has to be taken to make sure that the components are all completely clean. A speck of dried glue on one of the axles prevented a wheel from moving correctly, with it slipping rather than turning. This was immediately corrected.

4.3 Effect of the retractor unit on optical properties of the fibres

The next step will be to test a complete fibre bundle for focal ratio degradation (FRD). A fully characterised bundle consisting of 24 fibres³ is available for testing: 6 fibres will be put into a retractor, the others remain unused for comparison purposes. Of these 6 fibres, only 3 will be put through lifetime testing as described above, the other 3 will be checked for general wear and tear due to handling and installation/removal damage. The fibres that have been installed in the retractor and the fibres that have remained safely on the shipping drum will undergo a full re-measurement of the throughput and FRD characteristics of the individual fibres.

5. CURRENT MANUFACTURING STATUS

5.1 Commercial components

The main commercial components for the robotic positioner are the XYZ θ gantries with gripper units. These were prototyped and tested and an order was placed with Schunk GmbH & Co, with delivery expected in September 2016. The remaining commercial components have been delivered, including the tumbler motor and bearings, focal plane imager camera and various small optical components.

5.2 Manufactured components

The custom components of the positioner structure are currently being machined. The handling and assembly equipment is ready in the laboratory. Production of the rest of the positioner is currently 60% complete with completion scheduled by the time the robot gantries are delivered in September 2016.



Figure 12 WEAVE Handling and assembly trolley with positioner baseplate.

5.3 Fibre retractor units

The fibre retractor units described in the previous section have been tested as prototype units for several operational lifetimes and 360 production units have now been manufactured. The central aluminium plate and polycarbonate covers were all manufactured using CNC machines to achieve the accuracies required and as a result all parts are interchangeable. The pulleys, spring drums and attachment yokes are all injection moulded from ABS plastic. Each retractor unit has 58 individual components plus fasteners. Currently all components are complete with the central plates in the process of being anodised black.

6. TIMESCALES

The majority of the components of the positioner system are expected to be ready by the end of September 2016 with integration expected to be completed by the end of the year, followed by 6 months of testing and calibration using test fibres. The final stage will be the installation of the production fibre bundles in the tumbler system which will take an estimated 3 months, followed by some months of shakedown testing before shipping to the telescope in early 2018.

7. SUMMARY

We have described the current status of the positioner system for the WEAVE instrument for the prime focus of the William Herschel Telescope on La Palma. We have presented the results of technical prototyping of several key aspects of the instrument that are different to existing 2dF-like facilities.

REFERENCES

- [1] Gavin Dalton, et. al., “Project overview and update on WEAVE: the next generation wide-field spectroscopy facility for the William Herschel Telescope” in Ground-based and Airborne Instrumentation for Astronomy V, edited by by Suzanne K. Ramsay, Ian S. McLean, Hideki Takami, Proceedings of SPIE Vol. 9147 (SPIE, Bellingham, WA 2010) 91470L.
- [2] Gilbert, J., “New developments in robotic fibre positioning for astronomical multi-object spectroscopy,” Ph.D. dissertation, University of Oxford, 2016 (in press).
- [3] Frédéric Sayède, et. al., “First results of tests on the WEAVE fibres”, these proceedings, 2016